Numerical Study of Vorticity and Heat Flow in Bottom Heated DDC Systems at Nominal Rayleigh Number

N. Reddy[1†] and K. Murugesan[2]

[1] *Mechanical Engineering Department, SNIST, Hyderabad– 501301, India*
[2] *Mechanical & Industrial Engineering Department, Indian Institute of Technology Roorkee, Roorkee – 247 667, India*

†*Corresponding Author Email: dr.nithish.reddy@gmail.com*

ABSTRACT

Double diffusive convection (DDC) flows are widely seen in many industrial processes where the thermo-solutal buoyancy forces generates vorticity and initiates convective heat and mass transfer. In this paper numerical computations are conducted on this behaviour inside cavities of different aspect ratio at nominal Rayleigh number using a finite element based code. Velocity –vorticity form of Navier-Stokes equations are solved along with energy and solutal concentration conservation equations simultaneously using Galerkin's weighted residual method. Bottom wall is assumed hot and salted while top wall is maintained as sink, both side walls of the cavity are assumed to be adiabatic to heat and mass flow. Generally cavities with the present boundary conditions exhibit weak vorticity and convection characteristic especially at low Rayleigh number. In this numerical work an attempt is made to explore the role of variation in relative strength of thermal and solutal buoyancy forces on flow characteristics and mode of heat and mass transfer in such conditions. Simulation results have been reported for different buoyancy ratios in the range $-2 \leq N \leq 2$, Rayleigh number varying from 1.0e5 to 1.0e3, for cavities of aspect ratios, 0.5(shallow), 1 (square) and 2 (deep). Flow contours are well validated with the results in the literature. The fluid rotation patterns are captured and reported under different operating conditions chosen, the vorticity generation is observed relatively low for deep cavity when compared to other two. Investigations revealed that fluid convection gets greatly hampered when operated in negative buoyancy ratio regime and require relatively higher Rayleigh number to change the mode of heat transfer from diffusion to convection.

NOMENCLATURE

AR	aspect ratio		X, Y	non dimensional coordinates
C	concentration of species			
D	binary diffusion coefficient		α	thermal diffusivity
g	gravitational acceleration		β_C	concentration volumetric expansion coefficient
H	height of the cavity			
Le	Lewis number		β_T	thermal volumetric expansion coefficient
N	buoyancy ratio		μ	dynamic viscosity
Nu	local Nusselt number		υ	kinematic viscosity
Pr	Prandtl number		φ	non dimensional concentration of species
Ra	Rayleigh number		θ	non-dimensional temperature
Sc	Schmidt number		ρ	density
Sh	local Sherwood number		τ	non dimensional time
t	time		ω	vorticity
T	temperature		ς	non dimensional vorticity
u,v	horizontal and vertical velocity components		Δ	difference
U, V	non-dimensional velocity components			
U_0	lid velocity		**Subscripts**	
W	width of the cavity		av	average
x, y	horizontal and vertical coordinates		c	cold
			h	hot

1. INTRODUCTION

Buoyancy driven heat and fluid flow inside the cavities is one of the widely studied research subject over decades. A category of such natural convection phenomenon in bottom heated cavities under weak thermal buoyancy forces is popularly known as Rayleigh- Benard convection and thus formed convection cells are called Rayleigh – Benard cells(Pallsres *et al*. 1999; Quertatani *et al*. 2008). This phenomenon is further called Rayleigh-Benard thermo-solutal or double-diffusive convection when there exist simultaneous solutal diffusion along with heat in these systems. Presence of secondary diffusion generates solutal buoyancy forces which can either aid or oppose the growth of convection cells or cell vorticity. These double diffusive convection(DDC) problems find importance in natural phenomenon like convection in the oceans, earths outer core and in numerous geophysical phenomenon, also in many practical industrial processes like chemical vapour depositions, food processing, solidification and crystalline growth, lubrication in groves, solar distillation, cooling of electronic devices and so on (Nayak and Bhattacheryya 2012; Kumar *et al*. 2010). Because of their decent importance in the industries such flows are examined in multiple perspectives by the researchers till date. Kamotani *et al*. (1985) carried out an experimental investigations on DDC phenomenon in a low aspect ratio cavity. Their focus was on the formation of different flow structures and their importance in crystalline growth applications. Beghien *et al*.(1992) conducted a primary research on double diffusive natural convection in enclosures at Ra=1.0e7 . They gave the correlations for Nusselt and Sherwood number stating that solutal buoyancy forces can be aiding or opposing kind. Costa (1997) established a numerical model for the study of DDNC in enclosures. This model could effectively visualize the thermal and mass lines throughout the enclosure. The effect of solutal buoyancy forces on circulation phenomenon inside the cavity is another important aspect of the double diffusive convection. Nishimura *et al*. (1998) has conducted several numerical experiments with this perspective and concluded that increase in solutal buoyancy forces beyond certain level leads to oscillatory convection. Chen *et al*. (2010) worked on the effect of different operating parameters on DDNC flow inside an enclosure. They reported that multiple fluid cells are observed at higher Ra and N values, while at Ra=1.0e6 only single fluid cell is observed for all aspect ratios. Chouikh *et al*. (2007) investigated thermo-solutal convection in a rectangular cavity of aspect ratio 10 replicating a solar distiller model. They showed that the single circulation cell is favourable for allowing sufficient time for vapour to cool down. Han and Kuehn (1991) studied the nature of thermal and solutal buoyancy induced convection in differentially heated rectangular cavity of aspect ratio 4.They observed unicellular flow structure but could make any clear demarcation whether the case is of pure solutal dominant one or thermal dominant one. Alluoui *et*

al. (2010) modelled thermo-solutal convection in a very shallow enclosure considering Soret effect for a binary mixture subjected to solutal flux at horizontal boundaries. Mohamad *et al*. (2006) investigated natural convection in enclosure with cross thermal boundary conditions; they performed numerical analysis on floor cooling by varying the thermal conditions on the ceiling. From the results it is observed that the rate of heat transfer from the floor is a weak function of investigated parameters. Bouras *et al*. (2014) carried out numerical experiments on double diffusive natural convection in an elliptic shaped annuli filled with a Newtonian fluid using a new approach. From the results they demonstrated the potential of the proposed approach for such elliptical enclosures. Malekshah and salari (2017) conducted a natural convection study in a three dimensional enclosure filled with two immiscible fluids. They explored the convection characteristics at different height ratios of liquid to air and performed uncertainty analysis for the experimental data. Qin *et al*. (2014) succesfully analysed DDC in a rectangular cavity of aspect ratio 2 using compact difference method, Moufekkir *et al*.(2015) and Ren and Chan (2016) simulated double diffusive convection in vertical enclosures successfully using lattice Boltzmann method. Corcione *et al*. (2015) analysed heat and mass transfer rates in a differentially heated and salted square cavity case and gave the correlations of Nusselt number and Sherwood number. Nazari *et al*. (2015) and Kumar *et al*. (2011) focused on DDC in a square cavity model with a heated block inside. The conditions choosen here resembles some of the chemical engineering applications. From this numerical experiment they have reported optimum flow conditions for achieving maximum mass transfer rates. Oueslati *et al*.(2014) , Jenaa *et al*.(2015) and Nikbakhti *et al*.(2016) simulated double diffusive convection flows in cavities with partially heated and salted side walls and reported the flow structures under various operating parameters. Here they have underlined the significance of such flow structures in various application and process optimization. Maatki *et al*. (2016), Reddy and Murugesan (2017) studied the effect of magnetic field on double diffusive natural convection of binary fluid in a cubic cavity. From the results it is observed that with increase in inclination of the magnetic field in the direction of flow the hampering effect on the fluid convection is augmented. They also shown that depending on the Hartmann number the critical angle differs and major changes are noticed in flow structures at this stage. A part from regular conventional problems Bhadauria *et al*. (2016), studied double diffusive convection in couple stress fluid and Ayachi *et al*. (2010) conducted numerical experiments on double diffusive convection in porous media .

All the above works shows the importance of simulating and studying various aspects of double diffusive convection flows. The objective of the current study is to simulate the threshold limit of operating conditions for vorticity damping with simultaneous variation in different parameters like aspect ratio, buoyancy ratio, Rayleigh number etc..

Also, the results have importance for several applications where transport of heat and mass is of importance such as food processing, CVD, convection in freezers and other transport processes. Further, current problem is academically interesting for understanding the fundamentals of Rayleigh-Benard convection in presence of mass diffusion and the solutal forces. According to authors knowledge, study of the vorticity characteristics of chosen problem has not been explored by other people in such detail although the applications has been in practice from ancient times.

Here an attempt is made to numerically capture the vorticity and heat transfer patterns under nominal Rayleigh number in such poor convective cases by the solution to velocity-vorticity form of Navier-Strokes equations using finite element method. The interesting changes in the vorticity generation and transformations in heat transfer mode with change in balance between thermal to solutal buoyancy forces is recorded. Numerical studies are carried out for three different cavity aspect ratios in the nominal Rayleigh number regime i.e $1.0e3 \leq Ra \leq 1.0e5$. The relative strength of solutal to thermal buoyancy forces is given by buoyancy ratio parameter 'N" is varied in the range $-2 << \leq N \leq 2$ with six intervals in between.

2. GOVERNING EQUATIONS

Velocity vorticity form of Navier stokes equations are used to solve for flow field in the current work. (Kumar *et al.* 2011 ; Reddy and Murugesan 2017).

Vorticity transport equation can be written as

$$\frac{\partial \omega}{\partial t} + (V \cdot \nabla)\omega = \nu \nabla^2 \omega + \nabla \times \left[g\beta_T (T - T_\infty) \right] + \nabla \times \left[g\beta_c (C - C_\infty) \right] \tag{1}$$

where T is temperature, C is concentration, $\mathbf{V} = (u, v)$ are the velocity components in x and y directions respectively, ω is the vorticity component. and

$$\beta_T = -\frac{1}{\rho}\frac{\partial \rho}{\partial T}\bigg|_{p,C} \qquad \beta_C = -\frac{1}{\rho}\frac{\partial \rho}{\partial C}\bigg|_{p,T}$$

Here β_T and β_C are the thermal and solutal volumetric

expansion coefficients respectively.

To solve for the flow field, along with the above vorticity equations continuity has to be imposed. To do that we have another set of equations namely velocity Poisson equations .

$$\nabla^2 V = -\nabla \times \omega \tag{2}$$

For energy and solutal fields we have

Energy equation:

$$\frac{\partial T}{\partial t} + V.(\nabla T) = \alpha \nabla^2 T \tag{3}$$

Solutal concentration equation:

$$\frac{\partial C}{\partial t} + V.(\nabla C) = D\nabla^2 C \tag{4}$$

Equations (1),(2),(3) and (4) are the dimensional form of governing equations for double-diffusive natural convection in velocity-vorticity form.

The non-dimensional form of the above equations can be obtained by using the following scaling parameters .

Spatial coordinates, $X = x/L, Y = y/L$ velocities, $U = uL/\alpha$, $V = vL/\alpha$, vorticity, $\varsigma = \frac{\omega L^2}{\alpha}$,time= $\tau = \frac{\alpha t}{L^2}$, temperature $\Theta = T - T_c / T_h - T_c$

and solutal concentration $\phi = \frac{C - C_C}{C_h - C_C}$

After substituting the above scaling parameters the final governing equations in non-dimensional form can be written as

$$\frac{\partial \varsigma}{\partial \tau} + U\frac{\partial \varsigma}{\partial X} + V\frac{\partial \varsigma}{\partial Y} = \Pr\left(\frac{\partial^2 \varsigma}{\partial X^2} + \frac{\partial^2 \varsigma}{\partial Y^2}\right) + Ra\Pr\left(N\frac{\partial \phi}{\partial X} + \frac{\partial \theta}{\partial Y}\right) \tag{5}$$

$$\frac{\partial^2 U}{\partial X^2} + \frac{\partial^2 U}{\partial Y^2} = -\frac{\partial \varsigma}{\partial Y} \tag{6}$$

$$\frac{\partial^2 V}{\partial X^2} + \frac{\partial^2 V}{\partial Y^2} = \frac{\partial \varsigma}{\partial X} \tag{7}$$

$$\frac{\partial \theta}{\partial \tau} + U\frac{\partial \theta}{\partial X} + V\frac{\partial \theta}{\partial Y} = \frac{\partial^2 \theta}{\partial X^2} + \frac{\partial^2 \theta}{\partial Y^2} \tag{8}$$

$$\frac{\partial \phi}{\partial \tau} + U\frac{\partial \phi}{\partial X} + U\frac{\partial \phi}{\partial Y} = \frac{1}{Le}\left(\frac{\partial^2 \phi}{\partial X^2} + \frac{\partial^2 \phi}{\partial Y^2}\right) \tag{9}$$

where non-dimensional numbers are defined as, Rayliegh number $Ra = g\beta_T \Delta T H^3$ /

$Ra = \frac{g\beta_T \Delta T H^3}{\nu\alpha}$, buoyancy ratio $N = \beta_c \Delta C / \beta_T \Delta T = GR_s / GR_T$, Prandtl number, $Pr = \upsilon / \alpha$ and $Le = Sc / Pr$.

3. SOLUTION METHODOLOGY

Global matrix-free Galerkin's weighted residual finite element method is employed in solving the governing equations for velocity, vorticity, temperature and solutal concentration fields over entire domain. Velocity- Vorticity formulation helps in directly obtaining the desired primary parameters in vortex dominant flows with less computational cost. The computational domain is initially discretized into a number of bilinear isoparametric quadrilateral elements and for each

element the partial differential governing questions are approximated. Second order accurate Crank-Nicolson scheme is used in discretizing the time derivative. Governing equations at elemental level are formulated and are converted into algebraic form by integration using Gaussian quadrature method. The assembly procedure is completely eliminated in this work by implementing global matrix free finite element algorithm (Murugesan *et al*. 2006). The advantage of this algorithm is, in this procedure the element level matrices are not assembled to form global matrices, instead they are kept in element level itself, and then the boundary conditions are included at element level matrices for those elements contributing to the boundary nodes. Assembly of element level matrices is carried out only once at the time of solving the final simultaneous equations. This algorithm eliminates the storage of huge sparse matrices obtained as a result of assembly. The final simultaneous equations are solved by using conjugate gradient iterative solver (Press *et al*. 1992). Iterative procedure is continued until the error in all the field variables between successive iterations reduced below 1.0e−5. An in-house computer code developed in FORTRAN using global matrix-free finite element algorithm has been used to obtain the simulation results discussed in this work. The computer program was run on a Quad Core-Dual Xeon Processor Workstation with 2.0 GHz speed platform.CPU time varyied from 24-36 hours for each case based on operating parameters.
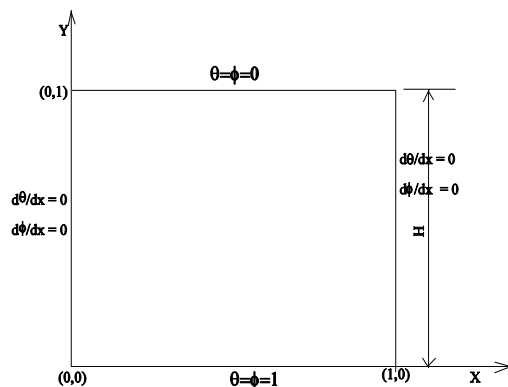
Problem Description

The schematic diagram of the problem domain is shown in Fig.1. A square cavity of height H with adiabatic and impermeable side vertical walls is considered for this study. The bottom wall is maintained hot and high species concentration, whereas top wall is assumed cold and low species concentration. No slip boundary conditions are assumed for velocity components on all the wall boundaries. The flow is assumed to be two-dimensional, simulations are carried out for different relative strength of thermal and solutal buoyancy forces in the cavity for three different aspect ratios 0.5, 1.0,2.0. Aspect ratio here is defined as ratio between non-dimensional height to
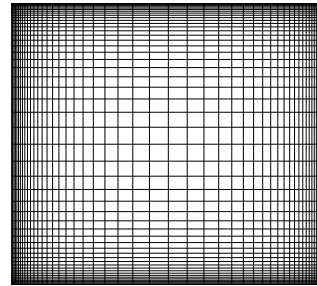
width of the cavity.

Fig. 2. Computational mesh.

Initial and boundary conditions:

Initial conditions:

@ $\tau=0$, $U=V=\Theta=\Phi=0$

Boundary conditions for $\tau>0$

$U=V=0$, $\Theta=1$, $\Phi=1$ *at Y=0 for 0<X<1*

$U=V=0$, $\Theta=0$, $\Phi=0$ *at Y=1 for 0<X<1*

$U=V=0, \dfrac{\partial\Theta}{\partial X}=0$, $\dfrac{\partial\Phi}{\partial y}=0$ at X=0 and X=1 for 0<Y<1

4. RESULTS AND DISCUSSION

4.1 Mesh Sensitivity Results

Non-uniform structured quadrilateral mesh is generated for the computational domain using transfinite interpolation (TFI) technique (See Fig. 2). From the experience of the authors it is found TFI is simple to control the non-uniformity at the boundary. In the case of velocity-vorticity formulation caliculation of vorticity

at the boundary are computed effectively using TFI technique. A mesh sensitivity test has been conducted using three different structured computational meshes M1 (71×&71),M2(51×51) and M3(41×41). The error between M2 and M3 is hardly 1% and is found decreased when compared to M1 and M2. Thus Mesh M2 is chosen for the current investigations.

4.2 Validation Results

Figure. 3 gives the comparison of present iso-therms ,iso-concentration and stream lines with that of the results obtained by Chamkha and Al-Nasar (2002) for a double diffusive natural convection case. Table 1 presents the quantitative comparison of corresponding average Nusselt number and average Sherwood number. It is observed that present results using velocity vorticity formulation are matching very well with that of the literature. Therefore the present FEM code is used for further investigations
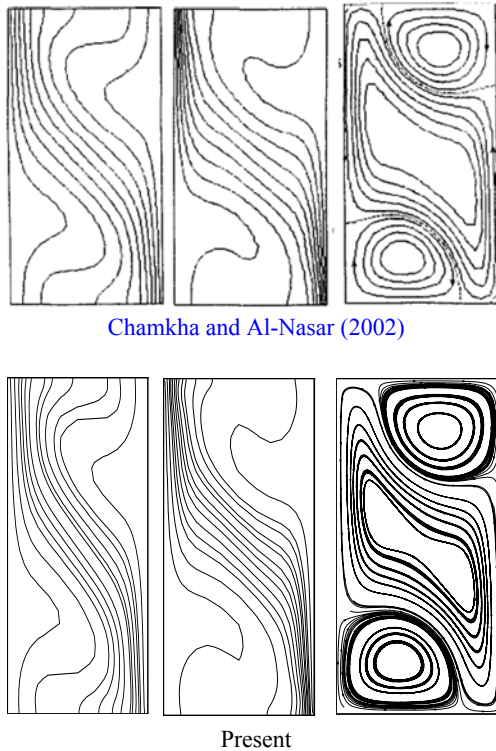
Fig. 1. Schematic diagram.

Chamkha and Al-Nasar (2002)

Present

Fig. 3. Iso-therms, iso-concentration and stream line comparisons at Ra=1.0e5, N=1.

Table 1 Comparison of the present results for Average Nu and Sh with that of Chamkha and Al-Naser (2002) at Ra=1.0e5,Pr =1,Le=2

	N=0.8		N=1.3	
	Nu	Sh	Nu	Sh
Chamkha and Al-Nasar (2002)	3.643	4.862	2.12	3.18
Present	3.594	4.814	`2.08	3.12

4.3 Simulation Results

In the current study numerical simulations were carried out for the bottom heated and salted cavity as shown in Fig. 1. Similar diffusion characteristics were assumed for both heat and mass transfer, simulations were conducted for different buoyancy ratios ranging from -2≤N≤2 , $1.0e3 \leq Ra \leq 1.0e5$,Le=1 for cavities of aspect ratios, 0.5 (shallow), 1 (square) and 2 (deep). Results obtained are presented in the various sections as follows

4.3.1 Effect of Buoyancy Ratio and Aspect Ratio on Fluid Flow

In this section results obtained for vorticity in case of square (AR=1.0), shallow (AR=0.5) and deep cavities (AR=2.0) are presented for Ra=1.0e5, 1.0e4, 1.0e3 and N=1, 0.5,-0.5,-1. At Ra=1.0e5 , Figs. 4a, 5a and 6a results shows that vorticity reduces drastically when buoyancy ratio parameter 'N' is marched in negative direction. Here one can notice that when buoyancy ratio is 1.0 fluid vorticity dropped close to zero, at this point heat and mass transfer takes place purely through diffusion. In contrast when buoyancy ratio is increased

in positive direction the fluid vorticity has shown increasing trend for all the three cavities. Maximum rotational strength is generated in case of shallow cavity followed by deep and square cavities. This may be a result of geometrical constraints on fluid rotational path. With change in aspect ratio of geometry circulation pattern is found uni cellular in case of square cavity, duel and tri cellular in case of shallow cavity, single, duel and tri all three types of circulations are observed in case of deep cavity when the balance between thermal and solutal buoyancy forces is varied. Multiple break down of vortices although aids local mixing of contaminates/solutal particles but they disturbs the uniformity which is essential in processes like chemical vapour deposition. Figs. 4b, 5b and 6b reports the vorticity contours in case of Ra=1.0e4, in this case hardly any vorticity is generated in shallow and deep cavities for all N values. In case of square cavity it is observed that vorticity drops down close to zero only when operated in negative buoyancy ratio regime. For positive buoyancy ratio regime with increase in 'N' value some increment in vorticity is recorded but is found relatively low when compared to Ra=1.0e5 case. Thus it can be said that to initiate the convective heat and mass transfer relatively higher Rayleigh number is essential for shallow and deep cavities when buoyancy forces are in limit of current proportions. In case of Ra=1.0e3 change in buoyancy ratio in both positive and negative direction has not shown any significant effect on fluid vorticity for all the three cavities. The vorticity here has not been initiated which says that driving forces are very weak and thus any imbalance between thermal and solutal buoyancy forces could not make any difference.

4.3.2 Effect of Buoyancy Ratio and Aspect Ratio on Thermal Field

In this section Figs. 7,8 and 9 presents iso-therms corresponding to square, shallow and deep cavities respectively for different buoyancy ratio and Rayleigh number. From results of Ra=1.0e5 case (see Figs. 7a, 8a and 9a) it is observed that Isotherms are found straight for N = 1.0 due to poor vorticity. Thermal gradients are observed steeper with increase in buoyancy ratio in positive direction indicating enhanced heat transfer. Distribution of isotherms with change in buoyancy ratio is observed similar for square and shallow cavities but in case of deep cavity a different trend is noticed for N=0.5 and 1.0 case. This may be due to multiple break down of strong vortices with change in buoyancy ratio. Figs. 7b,8b and 9b presents the case of Ra=1.0e4 for square ,deep and shallow cavities respectively. Here for all buoyancy ratios isotherms are observed straight in case of shallow cavity, similarly in case of deep cavity ,which indicates the poor convective transport. For square cavity isotherms are found straight for negative buoyancy ratio and curvy for positive buoyancy ratio due to vorticity enhancement. In case of Ra=1.0e3 (see Figs. 7c, 8c, 9c) isotherms are observed straight for all buoyancy ratio, aspect ratios indicating that buoyancy forces are not strong enough to generate fluid circulation.
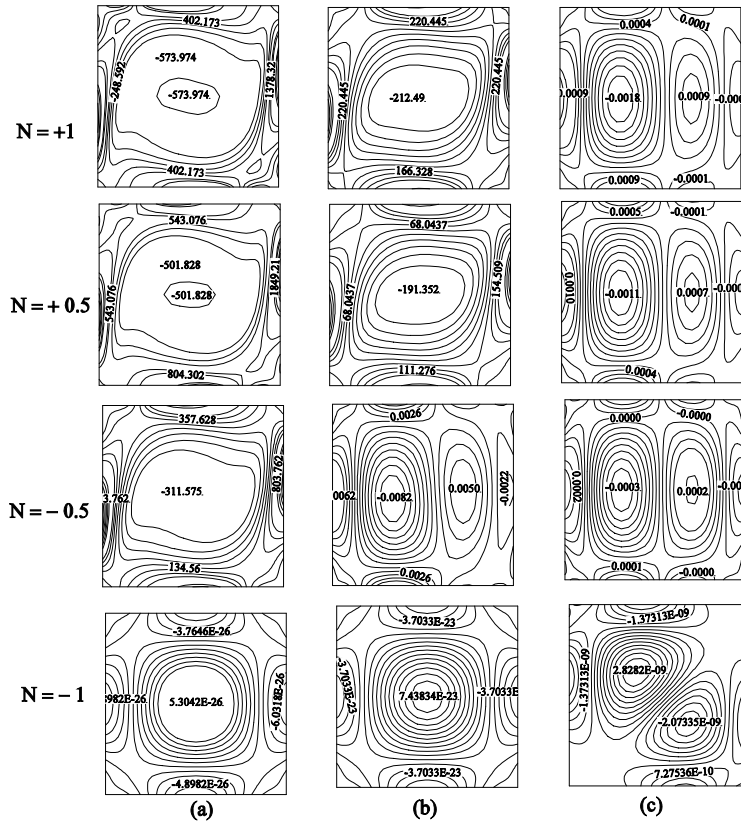
Fig. 4. Vorticity contours in a square cavity at different buoyancy ratios and Rayleigh numbers (a) Ra=1.0E05 (b) Ra=1.0E04 (c) Ra=1.0E03.
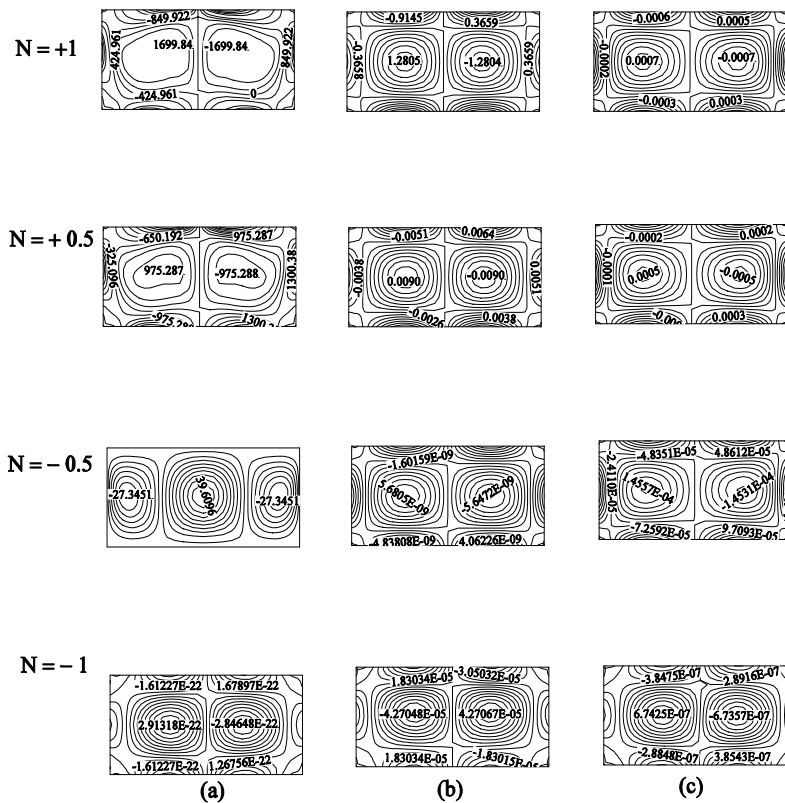

Fig. 5. Vorticity contours in a Shallow cavity(AR=0.5) at different buoyancy ratios and Rayleigh numbers (a) Ra=1.0E05 (b) Ra=1.0E04 (c) Ra=1.0E03.
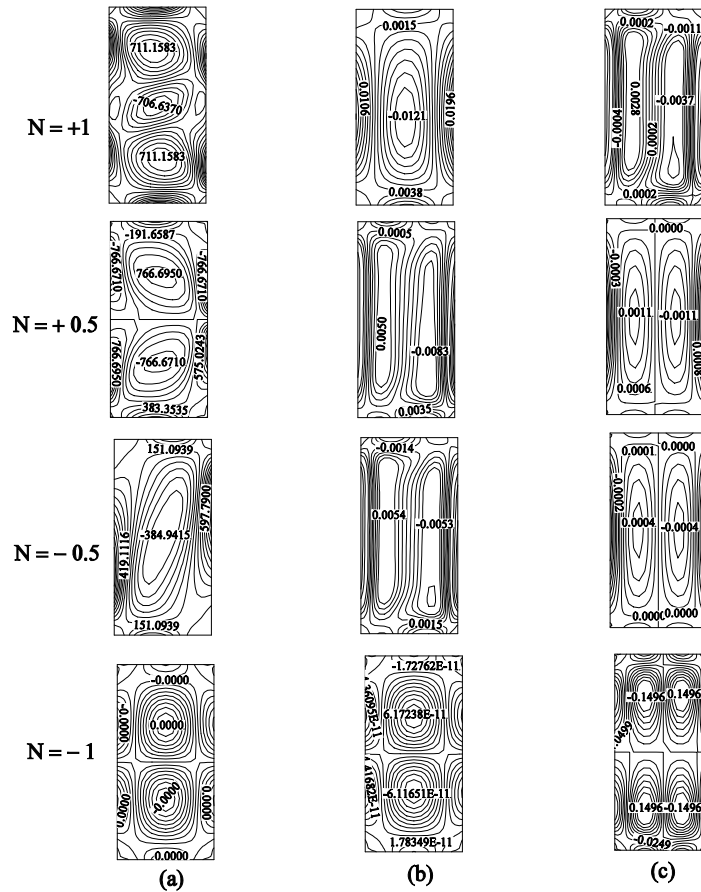
Fig. 6. Vorticity contours in a deep cavity(AR=2.0) at different buoyancy ratios and Rayleigh numbers (a) Ra=1.0E05 (b) Ra=1.0E04 (c) Ra=1.0E03.
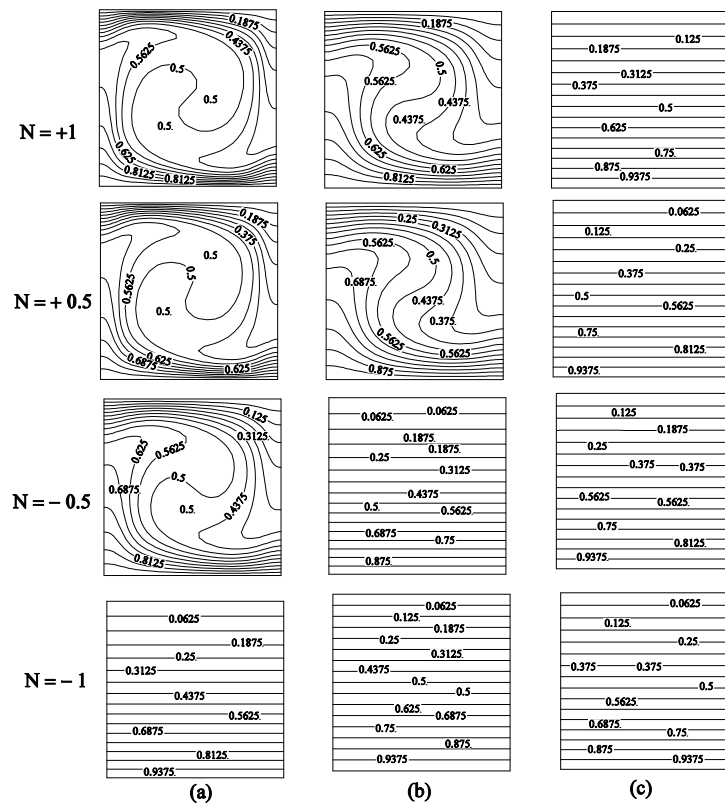

Fig. 7. Isotherms in a Square cavity at different buoyancy ratios and Rayleigh numbers (a) Ra=1.0E05 (b) Ra=1.0E04 (c) Ra=1.0E03.
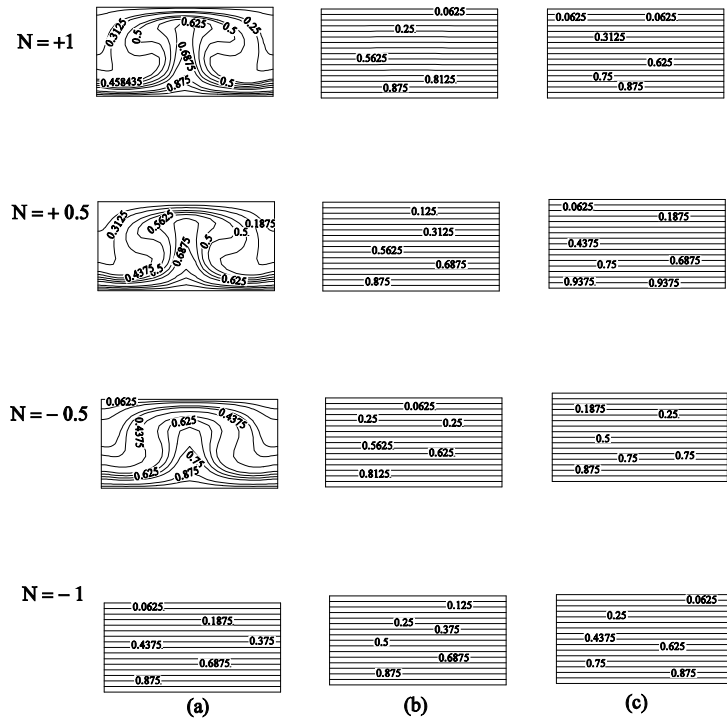
Fig. 8. Isotherms in a Shallow cavity(AR=0.5) at different buoyancy ratios and Rayleigh numbers (a) Ra=1.0E05 (b) Ra=1.0E04 (c) Ra=1.0E03.
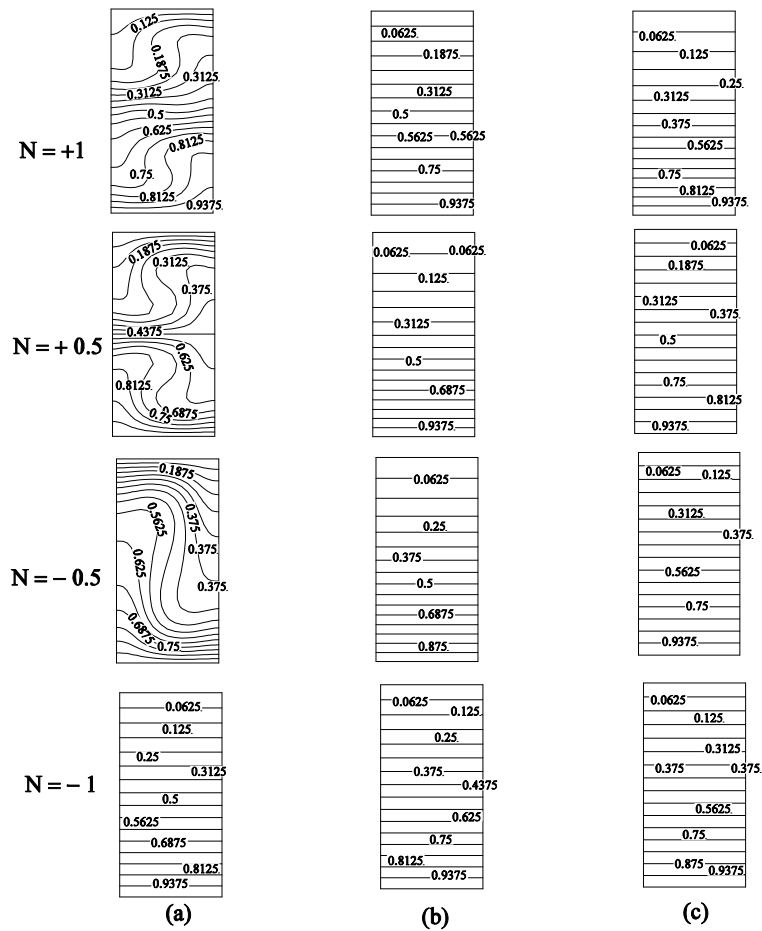

Fig. 9. Isotherms in a deep cavity(AR=2.0) at different buoyancy ratios and Rayleigh numbers (a) Ra=1.0E05 (b) Ra=1.0E04 (c) Ra=1.0E03.
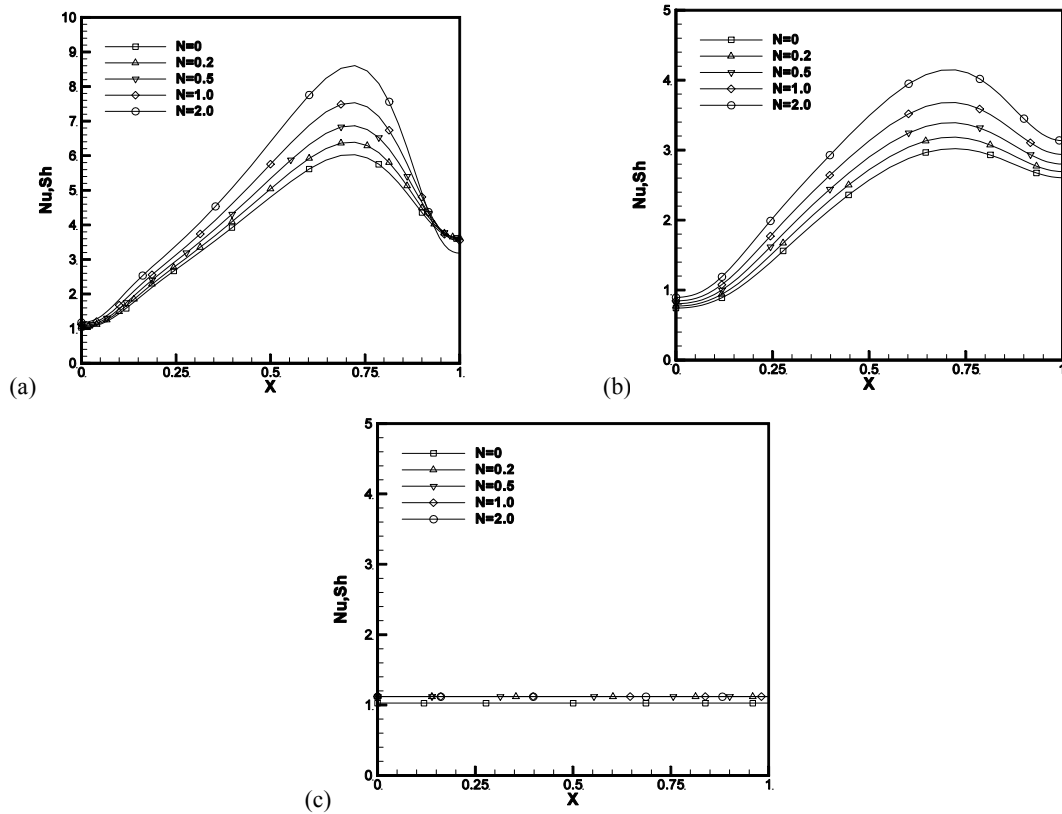
Fig. 10. Local Nusselt and Sherwood number along the bottom wall of square cavity for different buoyancy ratios in Positive regime at Rayleigh numbers (a)Ra=1.0E5 (b) Ra=1.0E4 (c) Ra=1.0E3.
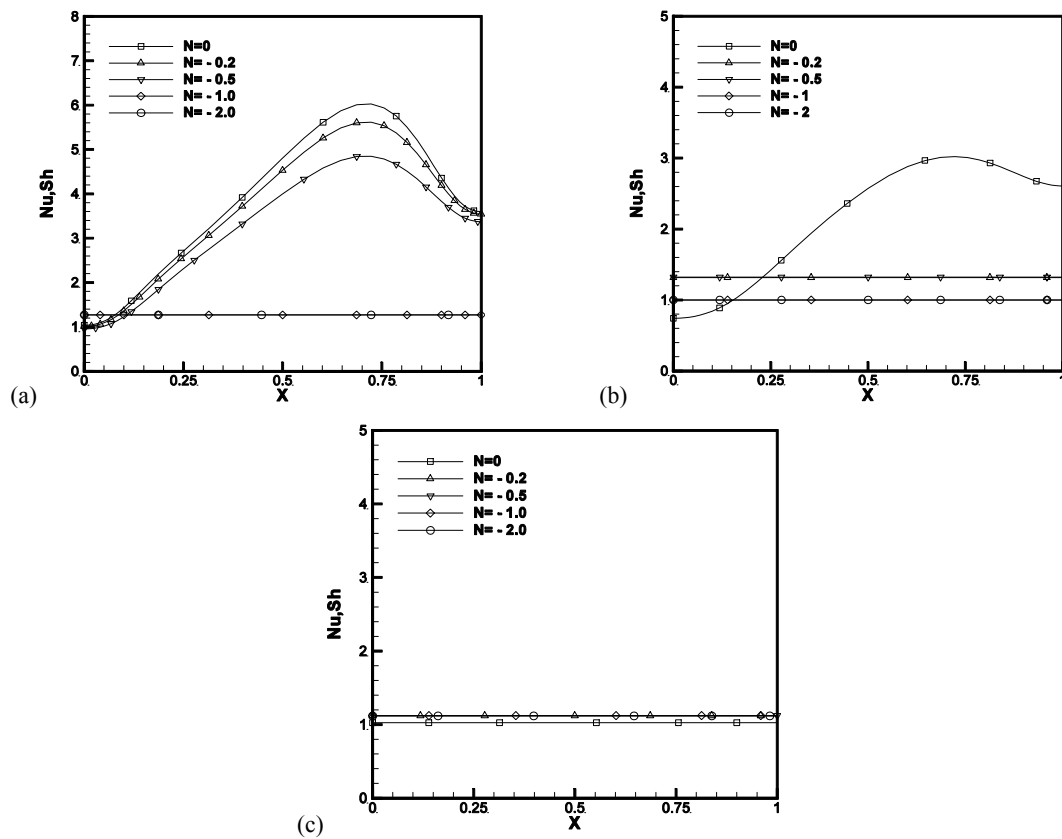

Fig. 11. Local Nusselt and Sherwood number along the bottom wall of square cavity for different buoyancy ratios in negative regime at Rayleigh numbers (a)Ra=1.0E5 (b) Ra=1.0E4 (c) Ra=1.0E3.
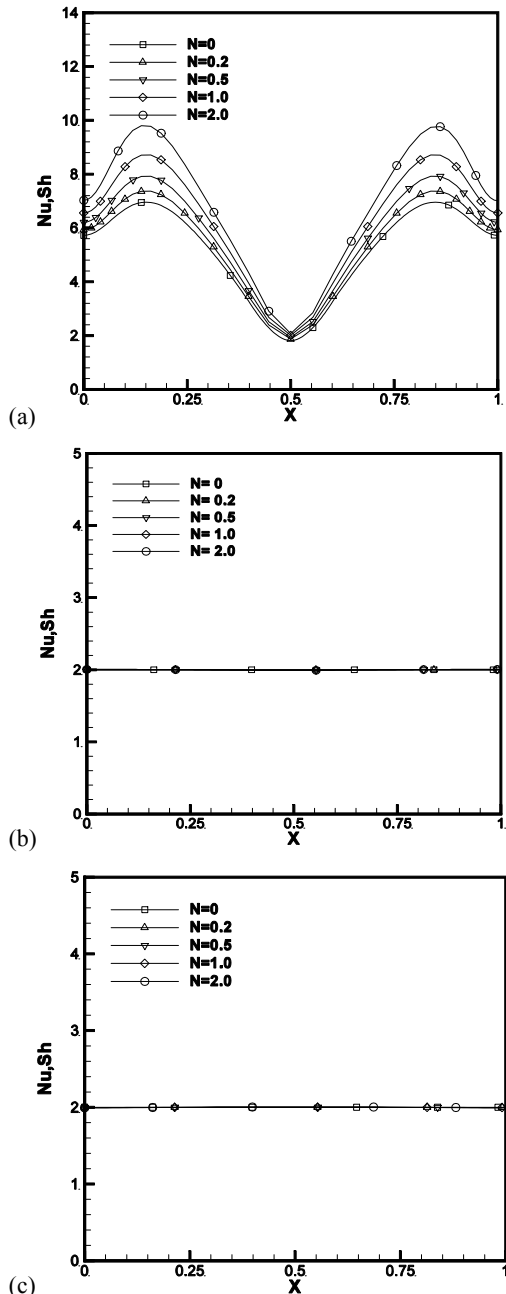
(a)

(b)

(c)

Fig. 12. Local Nusselt and Sherwood number along the bottom wall of shallow cavity(AR=0.5) for different buoyancy ratios in Positive regime at Rayleigh numbers (a)Ra=1.0E5 (b) Ra=1.0E4 (c) Ra=1.0E3.

4.3.3 Nusselt and Sherwood Number

In this section Nusselt number and Sherwood number calculated along the bottom wall are compared for various cases. Since similar heat and mass transfer characteristics are assumed for both thermal and solutal diffusion, Nusselt and Sherwood numbers showed similar trends. Figure. 10 describes the trend of local Nusselt number with change in buoyancy ratio in positive regime for different Rayleigh number when the cavity aspect ratio is 1 i.e for square cavity. From the plot it is observed that except at Ra=1.0e3 for both Ra=1.0e4

and 1.0e5 cases heat and mass transfer rates shown increasing trend with increase in buoyancy ratio. This confirms that increase in contribution of solutal buoyancy forces increases fluid convection inside the cavity. But at low Ra i.e at Ra=1.0e3 buoyancy forces are not strong enough to generate fluid circulation thus Nusselt number and Sherwood number lines are observed straight. Also the value of Nusselt number and Sherwood number confirms that the circulation is relatively stronger in case of Ra=1.0e5 compared to Ra=1.0e4 for all buoyancy ratios. For all values of N peak Nusselt number is observed at X=0.75, such variations in Nusselt number along the bottom wall are directly related to the fluid motion near bottom wall. Similarly Fig. 11 reports the results when operated in the negative buoyancy ratio regime. From the plot it is evident that Nusselt number and Sherwood number got hampered with increase in buoyancy ratio. In case of Ra=1.0e5 conduction mode dominated with increase in N to −1 and above, where as in case of Ra=1.0e4 such phenomenon is observed at N= −0.2. Here Nusselt number and Sherwood number lines are observed straight and horizontal with some difference in magnitude, such difference may be because of difference in fluid vorticity levels. At Ra=1.0e3 no change is observed in heat and mass transfer rates with increase in buoyancy ratio. Figure. 12 represents the case of cavity with aspect ratio 0.5 , here Nusselt and Sherwood numbers have not shown significant variation with change in buoyancy ratio except at Rayleigh number Ra=1.0e5. At Ra=1.0e5 increase in buoyancy ratio resulted in increase in Nu and Sh when operated in positive buoyancy ratio regime but when marched in negative buoyancy ratio regime heat transfer rate is decreased (see Fig. 13).In the case of deep cavity (see Fig. 14) with increase in buoyancy ratio heat transfer rate increased for only Ra=1.0e5 case, while for other two Rayleigh numbers no significant change is observed. For negative buoyancy ratios at Ra=1.0e5 (see Fig. 15) with decrease in buoyancy ratio below -0.5 heat transfer rate has reduced drastically. For Ra=1.0e3 and 1.0e4 heat transfer in deep cavity is observed by means of conduction alone (see previous section) and the buoyancy ratio has not played much role at these Rayleigh number for deep cavity.

4. CONCLUSIONS

Double diffusive natural convection in a bottom heated and salted cavity has been simulated numerically for different relative strengths of thermal and solutal buoyancy forces. Velocity-vorticity forms of Navier-Stokes equations are derived and solved numerically using finite element based code. Cavities of three different aspect ratios have been chosen and simulations are repeated for three Rayleigh numbers ranging from 1.0e5 to 1.0e3. Buoyancy ratio is varied from 2 to -2 and the variation in vorticity, mode of heat and mass transfer is reported for deep(AR=2) ,square(AR=1.0) and shallow(AR=0.5) cavities. Important research findings obtained from the analysis are presented as conclusions below:
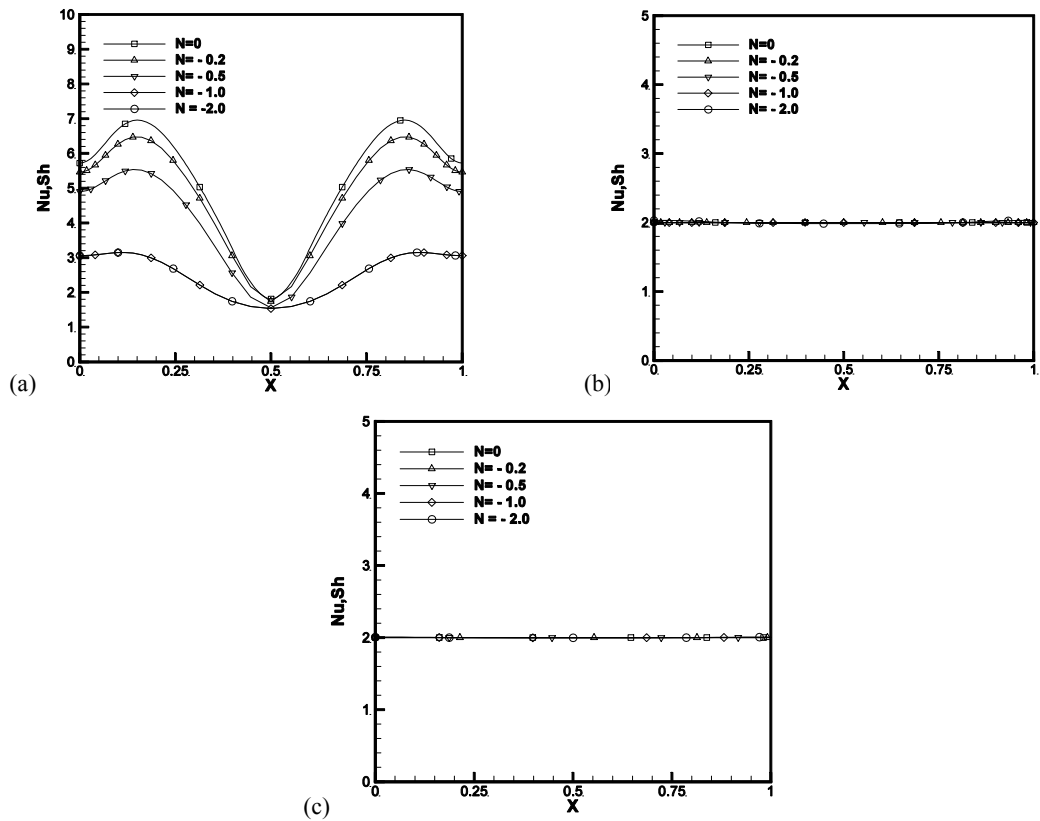
Fig. 13. Local Nusselt and Sherwood number along the bottom wall of shallow cavity(AR=0.5) for different buoyancy ratios in negative regime at Rayleigh numbers (a)Ra=1.0E5 (b) Ra=1.0E4(c) Ra=1.0E3.

Fig. 14. Local Nusselt and Sherwood number along the bottom wall of deep cavity(AR=0.5) for different buoyancy ratios in Positive regime at Rayleigh numbers (a)Ra=1.0E5 (b) Ra=1.0E4 (c) Ra=1.0E3.
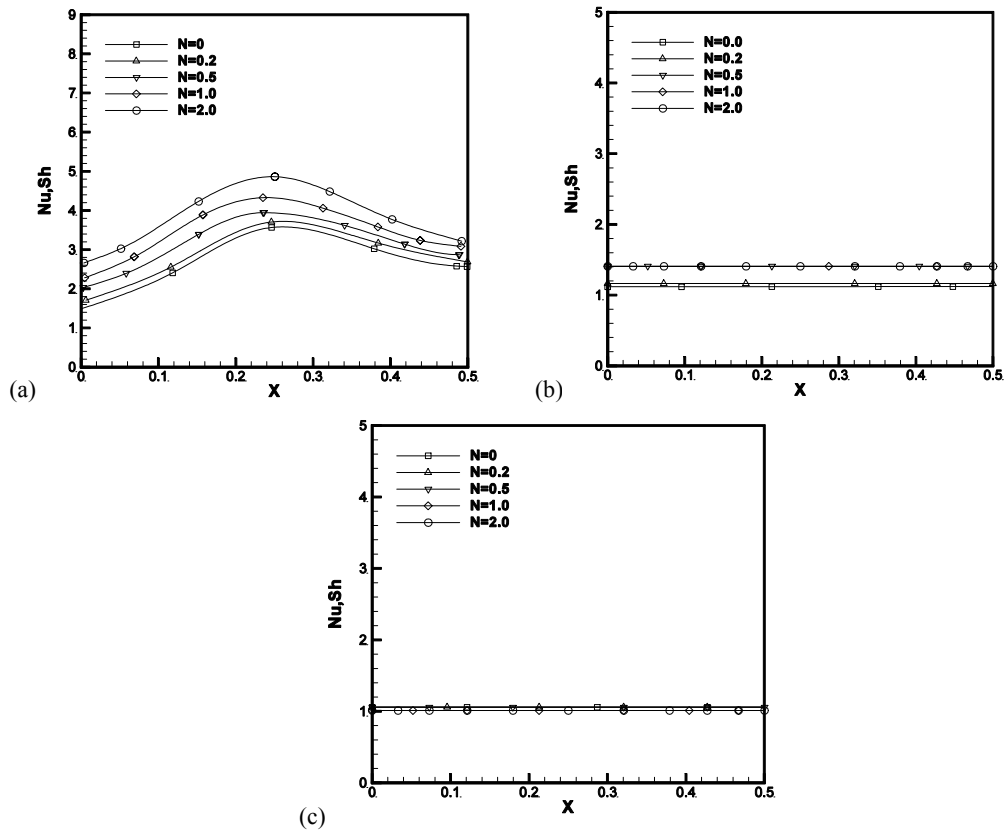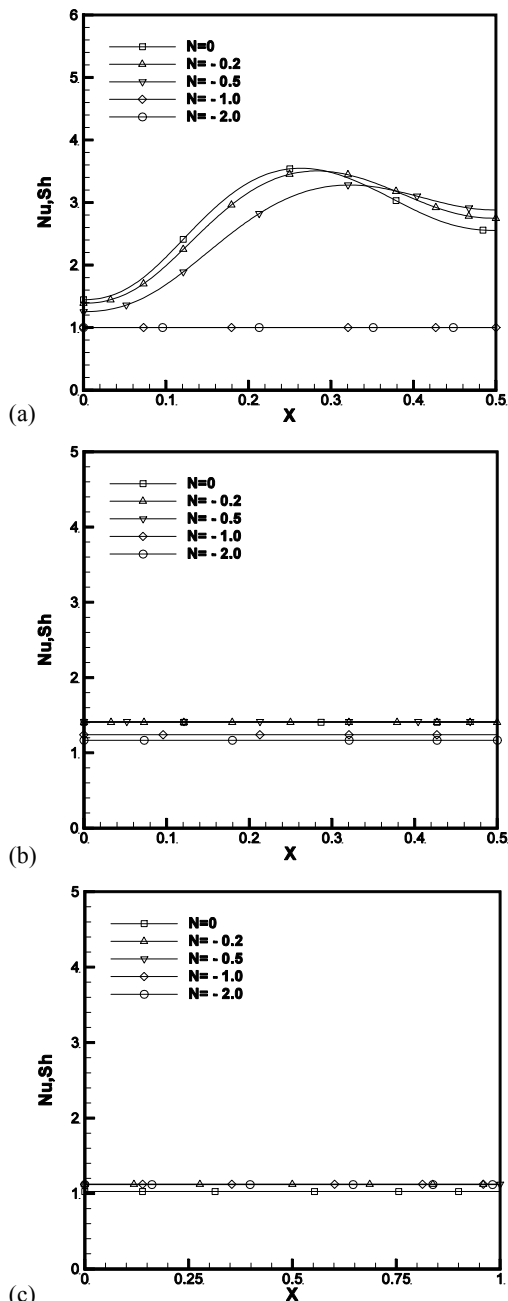
(a)

(b)

(c)

Fig. 15. Local Nusselt and Sherwood number along the bottom wall of deep cavity(AR=0.5) for different buoyancy ratios in negative regime at Rayleigh numbers (a)Ra=1.0E5 (b) Ra=1.0E4 (c) Ra=1.0E3.

- When the operating Rayleigh number is equal to 1.0e4 only square cavity is observed sensitive to change in buoyancy ratio and due to geometric constraints in the fluid flow path no significant change is observed in heat transfer rates in case of shallow and deep cavities.

- When buoyancy ratio is positive, with increase in value of 'N' vorticity strength in the cavities has improved and thus heat transfer rate has enhanced, this effect is felt more for Ra=1.0e5 where the degree

of convective forces is high.

- As 'N' is increased in negative direction fluid vorticity got hampered and heat transfer mode has shifted from convection to conduction even when operating Rayleigh number is equal to 1.0e5.

- At Ra=1.0e3, although buoyancy ratio could influence the circulation pattern but has not shown significant influence on heat transfer for any of the three aspect ratios considered.

- Fluid circulation pattern has been seriously affected with change in aspect ratio of the cavity. Interplay of thermo-solutal buoyancy forces resulted in unicellular in case of square cavity ,bi cellular in case of shallow and deep cavity shown all uni, bi and tri cellular rotations with change in buoyancy ratio at Ra=1.0e5.

- Fluid vorticity has reduced with increase in aspect ratio from 1 to 2 and opposite happened with decrease in aspect ratio to 0.5. Heat transfer rate is observed relatively weaker for deep cavity and higher for shallow one where the thermal boundaries are relatively closer

REFERENCES

Alloui, I., H. Benmoussa and P. Vasseur (2010). Soret and thermosolutal effects on natural convection in a shallow cavity filled with a binary mixture, *Int. J. Heat Fluid Flow* 31, 191–200.

Ayachi, R. E., A. Raji, M. Hasnaoui, A. Abdelbaki and M. Naimi (2010). Resonance of double-diffusive convection in a porous medium heated with a sinusoidal exciting temperature, *Journal of Applied Fluid Mechanics* 3(2), 43-52.

Bhadauria, B. S., P. G. Siddheshwar, A. K. Singh and K. G. Vinod (2016). A local nonlinear stability analysis of modulated double diffusive stationary convection in a couple stress liquid", *Journal of Applied Fluid Mechanics* 9(3), 1255-1264.

Bouras, A., M. Djezzar, H. Naji and C. Ghernoug (2014). Numerical computation of double-diffusive natural convective flow within an elliptic-shape enclosure, *In International Communications in Heat and Mass Transfer* 57, 183-192.

Chamkha, A. J. and H. Al-Naser (2002). Hydromagnetic double-diffusive convection in a rectangular enclosure with opposing temperature and concentration gradients, *Int. J. Heat Mass Transfer* 45, 2465–2483.

Chen, S., J. Tolke and M. Krafczyk (2010).

"Numerical investigation of double-diffusive (natural) convection in vertical annuluses with opposing temperature and concentration gradients", *Int. J. Heat Fluid Flow* 31, 217–226.

Chouikh, R., L. B. Snoussi and A. Guizani (2007). Numerical study of the heat and mass transfer in inclined glazing cavity:Application to a solar distillation cell, *Renewable Energy* 32, 1511–1524.

Corcione, M., S. Grignaffini and A. Quintino (2015). Correlations for the double-diffusive natural convection in square enclosures induced by opposite temperature and concentration gradients, *Int. J. Heat and Mass Transfer* 81, 811–819.

Costa, V. A. F. (1997). Double diffusive natural convection in a square enclosure with heat and mass diffusive walls", *International Journal of Heat and Mass Transfer* 40(17), 4061-4071.

Han, H. and T. H. Kuehn (1991). Double diffusive natural convection in a vertical rectangular enclosure- II, Numerical study", *Int. J. Heat Mass Transfer* 34(2), 461-471.

Jenaa, S. K., S. K. Mahapatra, A. Sarkar and A. J. Chamkhac (2015). Thermo-solutal buoyancy-opposed free convection of a binary Ostwald–De Waele fluid inside a cavity having partially-active vertical walls, *Journal of the Taiwan Institute of Chemical Engineers* 51, 9–19.

Kamotani, Y., L.W.Wang, S. Ostrach and H. D. Jiang (1985).Experimental study of natural convection in shallow enclosures with horizontal temperature and concentration gradients, *Int. J. Heat Mass Transfer* 28(1), 165-173.

Kumar, S. D., M. Krishan and A. Gupta (2010). Numerical analysis of interaction between inertial and thermo-solutal buoyancy forces on convection heat transfer in a lid driven cavity, *ASME. J. Heat transfer* 132, 112501-1.

Kumar, S. D., M. Krishan and H. R. Thomas (2011). Effect of the aspect ratio of a heated block on the interaction between inertial and thermosolutal buoyancy forces in a Lid-Driven Cavity, *Numerical Heat Transfer Part A, pp. Applications* 60, 7604-628.

Maatki, C., W. Hassen, L.Kolsi, N. AlShammari, B. M. Naceur and H. B. Aissia (2016). 3-D Numerical study of hydromagnetic double diffusive natural convection and entropy generation in cubic cavity, *Journal of Applied Fluid Mechanics* 9(4), 1915-1925.

Malekshah, E. H. and M. Salari (2017). Experimental and numerical investigation of natural convection in a rectangular cuboid filled by two immiscible fluids, *Experimental Thermal and Fluid Science* 85, 388-398.

Mohamad,A. A., J. Sicard and R. Bennacer (2006).

Natural convection in enclosures with floor cooling subjected to a heated vertical wall, *In International Journal of Heat and Mass Transfer* 49, 108-121.

Moufekkir, F., M. A. Moussaoui, A. Mezrhab and H. Naji (2015). Study of coupled double diffusive convection–radiation in a tilted cavity via a hybrid multi-relaxation time-lattice Boltzmann-finite difference and discrete ordinate methods, *Heat and Mass Transfer* 51(4), 567–586.

Murugesan, K., D. C. Lo, D. L. Young, C. M. Fan and C. W. Chen (2006). Global matrix-free finite-element scheme for natural convection in a square cavity with step blockage, N*umerical Heat Transfer, Part B, Fundamentals* 50, 353–373.

Nayak, A. K. and S. Bhattacharyya (2012). Double-diffusive convection in a cubical lid-driven cavity with opposing temperature and concentration gradients, *Theor. Comput, Fluid Dyn.* 26, 565–581.

Nazari, M., L. Louhghalam and M. H. Kayhani (2015). Lattice Boltzmann simulation of double diffusive natural convection in a square cavity with a hot square obstacle, *Chinese Journal of Chemical Engineering* 23, 22–30.

Nikbakhti, R. and J. Khodakhah (2016). Numerical investigation of double diffusive buoyancy forces induced natural convection in a cavity partially heated and cooled from sidewalls, *Engineering Science and Technology an International Journal* 19(1), 322-327.

Nishimura, T., M. Wakamatsu and A. M. Morega (1998).Oscillatory double-diffusive convection in a rectangular enclosure with combined horizontal temperature and concentration gradients, *Int. J. Heat Mass Transfer* 41(11), 1601-1611.

Oueslati. F., B. Ben Beya and T. Lili (2014). Numerical investigation of thermosolutal natural convection in a rectangular enclosure of an aspect ratio four with heat and solute sources, *Heat and Mass Transfer* 50(5), 721–736.

Pallsres, J., F. X. Grau and F. Giralt (1999). Flow transitions in laminar Rayleigh-Bénard convection in cubical cavity at moderate Rayleigh numbers, *Int. J. Heat Mass Transfer* 42, 753–769.

Press, W. H., S. A. Teukolsky, W. T. Vetterling and B. P. Flannery (1992). Numerical Recipes in Fortran 77(1), 77-82.

Qin. Q., Z. A. Xia and Z. F. Tian (2014). High accuracy numerical investigation of double-diffusive convection in a rectangular enclosure with horizontal temperature and concentration Gradients, *Int. J. Heat Mass Transfer* 71, 405–423.

Quertatani, N., N. B. Cheikh, B. B. Beya and T. Lili

(2008). Numerical simulation of two dimensional Rayleigh-Bénard convection in an enclosure, *Comptes Rendus Mecanique* 336, 464–470.

Reddy, N. and K. Murugesan (2017). Finite element study of ddnc in bottom heated enclosures with mass diffusive side walls, *Frontiers in Heat and Mass Transfer* 8 – 003007.

Reddy, N. and K. Murugesan (2017). Magnetic field influence on double-diffusive natural convection in a square cavity – a numerical study, *Numerical heat transfer, part A: Applications* 71(4), 2017.

Ren, Q. and C. L. Chan (2016). Numerical study of double-diffusive convection in a vertical cavity with Soret and Dufour effects by lattice Boltzmann method on GPU , *Int. J. Heat and Mass Transfer* 93, 538-553.